



# An Improved Technique for Ear Recognition Based On Force Field Analysis and Convergence Analysis

Rajnish Pandey<sup>1</sup>, Shashank Shekhar Tiwari<sup>2</sup>, K K Gupta<sup>3</sup>

<sup>1</sup>Department of Information Technology, Dr. RMLA University,  
Faizabad, UP, India

<sup>2</sup>Department of Computer Science & Engineering, Dr. APJ Abdul Kalam Technical University,  
Lucknow, UP, India

<sup>3</sup>Department of Computer Science, Dr. RMLA University,  
Faizabad, UP, India

## ABSTRACT

Ear recognition based on the force field transform is new and effective. Three different applications of the force field transform were discussed in this paper. Firstly, we discussed the problem in the process of potential wells extraction and overcame the contradiction between the continuity of the force field and the discreteness of intensity images. Secondly, an improved convergence-based ear recognition method was presented in this paper. To overcome the problem of threshold segmentation, an adaptive threshold segmentation method was used to find the threshold automatically; to reduce the computational complexity, a quick classification was realized by combining the Canny-operator and the Modified Hausdorff Distance (MHD). Finally, the algebraic property of force field was combined with Principal Component Analysis (PCA) and Linear Discriminant Analysis (LDA) together to obtain feature vectors for ear recognition. We tested these applications of the force field transform on two ear databases. Experimental results show the validity and robustness of the force field transform for ear recognition.

**Keywords:** Ear Recognition, Force-Field Transform, Convergence Feature Extraction, Adaptive Threshold Segmentation, Modified Hausdorff Distance

## I. INTRODUCTION

Earlier research has shown that human ear is one of the representative human biometrics with uniqueness and stability. At present, ear feature extraction methods for 2D intensity images could be roughly divided into two categories: one is based on the entire feature, and it projects the original n-dimensional data onto the k-dimensional subspace, such as the Principal Component Analysis <sup>1</sup> (PCA); the other is based on the local feature, such as the long axis based shape and structural feature extraction method <sup>2</sup> and the force field transform method <sup>3-5</sup>. Among these methods, the force field transform method is robust and reliable with remarkable invariance to initialization, translation and scaling and possessing excellent noise tolerance, so it is thought to be promising in the field of ear recognition.

Feature extractions based on the force field transform could be divided into two categories: force field feature extraction and convergence feature extraction. As for the first feature extraction method, researchers hope to find the potential wells as features for a subject. But it is quite possible that several ear images have less than



two potential wells so that the number of potential wells is not enough for classification. Hence, Hurley presented the convergence feature extraction method<sup>5</sup> for ear recognition: firstly, he transformed the original image into the convergence image; secondly, he transformed the convergence images into binary images; finally, the template matching method is used to find the near neighbour for classification. However, this method is time consuming because the threshold for the convergence image is based on the experimental results, which is not only complicated but also lack of automaticity. To improve the automaticity and calculation speed of the convergence feature extraction, we presented an improved convergence-based ear recognition method. It adopted an adaptive threshold segmentation method to find the threshold for convergence map automatically. Instead of the template matching method, the Modified Hausdorff Distance was used to calculate the nearest neighbour for classification. Furthermore we also used the algebraic property of the force field for ear recognition.

The rest of the paper is organized as follows: Section 2 describes principles of the force field transform. We describe the force field feature extraction method in Section 3. In Section 4, the improved convergence feature extraction method is described. A variety of experimental results are presented in Section 5. Finally, we provide some concluding remarks in Section 6.

**II. ALGORITHM PRINCIPAL**

**2.1 Definition of force field**

There is a basic hypothesis for the force field transform: each pixel in the image can exert an isotropic force on all the other pixels that is proportional to pixel intensity and inversely proportional to the square of the distance<sup>3</sup>. Therefore, the total force exerted on a pixel of unit intensity at the pixel location is the vector sum of all the forces due to the other pixels in the image. According to the basic hypothesis for the force field transform, the pixels are considered to attract each other according to the product of their intensities and inversely to the square of the distances between them. Each pixel is assumed to generate a spherically symmetrical force field so that the total force  $F(r_j)$  exerted on a pixel of unit intensity at the pixel location with position vector  $r_j$  by a remote pixels with position vector  $r_i$  and pixel intensities  $P(r_i)$  is given by the vector summation<sup>3</sup>, shown in the equation (1). To calculate the force field for the entire image, this equation should be applied at every pixel position in the image. Fig. 1(b) shows the magnitude of a force field that has been generated from an ear image Fig. 1(a).

$$F(r_j) = \sum_{i=1}^N F_i(r_j) = \sum_{i=1}^N P(r_i) \times (r_i - r_j) / |r_i - r_j|^3 \quad (\forall i \neq j) \tag{1}$$

**2.2. Definition of convergence field**

The force is a vector, while the convergence field is a scalar. If we calculate the divergence of the force field, the convergence field could be got, and the vector could be translated into the scalar. The divergence of a vector field is a differential operator that produces a scalar field representing the net outward flux density at each point in the field. For the vector force field  $F(r)$  it is defined as<sup>5</sup>,

$$c(r) = -divf(r) = \left( \frac{\delta f_x}{\delta x} + \frac{\delta f_y}{\delta y} \right) \tag{2}$$

$$f(r) = F(r) / |F(r)| \tag{3}$$

This function maps the force field to a scalar field, taking the force as input and returning the additive inverse of the divergence of the force direction.  $C(r)$  is the force direction convergence field or just convergence for brevity. The convergence is just another description for force field. Fig. 1(c) shows the magnitude of a convergence field that has been generated from an ear image Fig. 1(a).

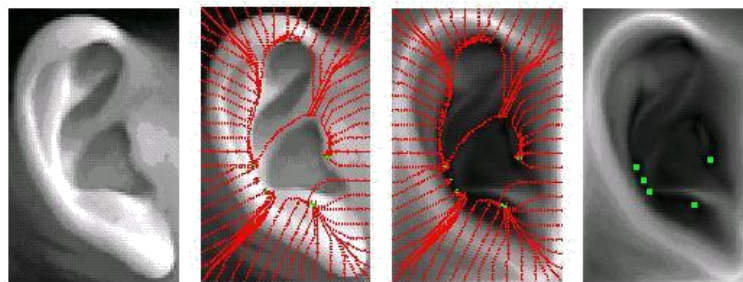


(a) Original image (b) Force field magnitude image (c) Convergence image

**Fig. 1. The results of force field transform and convergence feature extraction**

### III. FORCE FIELD FEATURE EXTRACTION

If an array of unit value exploratory mobile test pixels is arranged in a closed loop formation surrounding the target ear, each test pixel will be allowed to follow the pull of the force field so that its trajectory forms a field line and it will continue moving until it reaches the centre of a well where no force is exerted and no further movement is possible. In the Fig. 2, we arranged 62 test pixels around the original image, and these test pixels form the field lines (the red lines in Fig. 2(b), Fig. 2(c)) and potential wells (the green clusters of test pixels in Fig. 2(d)). The locations of these wells are extracted by simply noting the coordinates of the clusters of test pixels that eventually form. These locations are shown in Fig. 2(d), superimposed on force field magnitude. In order to smooth the field lines, we regulated the number of moving directions as eight. For the horizontal and vertical moving directions, the increment of each step for test pixels is half of the pixel space distance, while for the rest directions, half of the diagonal pixels space distance.



(a) (b) (c) (d)

**Fig. 2. Field lines and potential wells**

However, force exerted on test pixels is a continuity vector, while the locations of test pixels are discrete magnitude, so it is possible that the locations of potential wells are not in the track of the field lines. Therefore, this paper marked the locations of each step for a field line and chose the position where the test pixel moved forth and back as the finally potential well for such test pixel.



**IV. IMPROVED CONVERGENCE FEATURE EXTRACTION**

**4.1 Adaptive threshold segmentation for convergence images**

Hurley found out the threshold for each convergence image by experiment <sup>5</sup>, so it needs to adjust the threshold again and again manually until it could content the visual requirement. Hence it cannot be used directly on large databases. In this paper, an adaptive threshold segmentation was presented to select the threshold for convergence images automatically.

Assume there are L-gray levels for an image with N pixels. Let  $n_i$  be the number of pixels with  $i$  gray value. The threshold  $t$  will divide the image into two parts: the foreground and the background. Let the number of pixels in the background be  $N_1$  and that in the foreground be  $N_2$ . Hence the probability of background is  $P_1 = N_1/N$  and the probability of foreground is  $P_2 = N_2/N$ . Let the probability of different gray values in the image be  $h_i = n_i/N$ . The probability of different gray values in the background and that in the foreground is equation (4) and (5) respectively.

$$h_i^1 = \frac{n_i}{N_1}, i = 1, 2, \dots, t \tag{4}$$

$$h_i^2 = \frac{n_i}{N_2}, i = t + 1, \dots, L \tag{5}$$

Therefore, the gray center of the background, the gray center of the foreground and that of the whole image are defined in equation (6), (7) and (8) as  $m_1$ ,  $m_2$  and  $m$  correspondingly.

$$m_1 = \sum_{i=1}^t i h_i^1 = \sum_{i=1}^t i \frac{n_i}{N_1} \tag{6}$$

$$m_2 = \sum_{i=t+1}^L i h_i^2 = \sum_{i=t+1}^L i \frac{n_i}{N_2} \tag{7}$$

$$m = \sum_{i=1}^L i h_i^1 \tag{8}$$

Viewing the foreground and the background as two classes, the square of intra-class distance  $S_b^2(t)$  and the square of inner-class distance  $S_w^2(t)$  are defined in the equation (9) and (10) respectively.

$$S_b^2(t) = P_1(m_1 - m)^2 + P_2(m_2 - m)^2 \tag{9}$$

$$S_w^2(t) = P_1 \sum_{i=1}^t (i - m_1)^2 h_i^1 + P_2 \sum_{i=t+1}^L (i - m_2)^2 h_i^2 \tag{10}$$

So, the threshold is defined as the max ratio of intra-class and inner-class, defined in the equation (11).

$$J_f(t) = S_b^2(t)/S_w^2(t) \Rightarrow \max \tag{11}$$

Since pixels in the foreground focus on those that of high gray values, the threshold  $t$  must be on the right part of the histogram of each convergence image. We then use the ergodic algorithm to find the threshold for the converge image.

The results of using the adaptive threshold segmentation on one subject of USTB ear database was shown in the Fig. 3. More detailed description about the USTB ear database could be seen in the Sec. 5.1. Our threshold segmentation could extract enough foreground pixels from the background pixels, and the threshold segmentation results are almost close in different samples of the same subject, as shown in the Fig. 3.

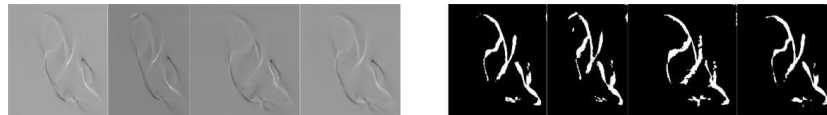


Fig. 3. Some results of using the adaptive threshold segmentation

### 4.2 Classification and recognition

After obtaining the binary image from the convergence image, Hurley used the template matching method for classification. However, this method is time consuming. In order to speed up the computing process, this paper adopted a new method which combined the canny operator with the Modified Hausdorff Distance <sup>6</sup> (MHD) to find the nearest neighbour as the basis for classification.

Unlike most shape comparison methods, the Hausdorff Distance (HD) can be calculated without the explicit pairing of points in their respective data sets, A and B. This paper adopted the MHD instead of HD simply because the former is

less sensitive to the noisy points (isolated points) than the latter. Formally, given two finite point sets  $A=\{a_1, a_2, \dots, a_m\}$  and  $B=\{b_1, b_2, \dots, b_n\}$ , the MHD is defined as equation(12).  $\|\cdot\|$  is some underlying norm over the point sets A and B. In this paper, we assume that the distance between any two data points is defined as the Euclidean distance.

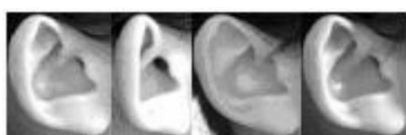
$$H_{MHD}(A,B) = \max[h_{MHD}(A,B), h_{MHD}(B,A)] \tag{12}$$

$$h_{MHD}(A,B) = \frac{1}{N_A} \times \sum_{a \in A} \min \|a - b\| \quad h_{MHD}(B,A) = \frac{1}{N_B} \times \sum_{b \in B} \min \|b - a\| \tag{13}$$

## V. EXPERIMENTAL RESULTS

### 5.1 Ear databases-

In this study, two ear databases were tested. The first one is from the Technical University of Madrid of Spain, just Spain ear database <sup>7</sup> for short. The second one is collected by our research group with various illumination and pose, named USTB ear database for short. Both ear databases are consisted of 8-bit gray images. There are 17 subjects with 6 different ear samples for each in the Spain ear database and 77 subjects with 4 different ear samples for each in the USTB ear database. Fig. 4 shows two subjects from different ear databases respectively.



(a) USTB ear database



(b) Spain ear database

Fig. 4. Ear databases. Fig. 4(a) is one subject from the USTB ear database. The leftmost ear image in the Fig. 4(a) was captured from front side with light off, compared to the rightmost one with light on. The second left ear image has +30 degree deflection from front side, while the third left one has -30 degree deflection from front side. Figure 4(b) is one subject from the Spain ear database with slight change of illumination and pose.

**5.2 Experimental procedure-**

In order to improve the speed of calculation, original images were resized to 48 ×30 pixels. After that, the force field feature extraction and the improved convergence feature extraction could be used.

In the process of force field extraction, we treated the magnitude of force field and the potential wells as two different kinds of features for ear recognition. The former one was combined with the Principal Component Analysis (PCA) and Linear Discriminant Analysis (LDA) to reduce the dimension and then the new ear image was identified by a nearest neighbour classifier. We call this method as F+PCA+LDA for short. The steps of obtaining potential wells for an original image could refer to the Sec. 3 or Ref. 4.

On the other hand, the ear recognition using improved convergence feature extraction has four steps. Firstly, using the force field transform to calculate forces of all pixels and after that, translate the original images into the convergence images; then the adaptive threshold segmentation was used to translate convergence images into binary images; thirdly, using the canny operator to extract the edge of each binary image and then form the edge points as a feature vector for this sample; finally, the new ear image was identified by a nearest neighbour classifier with MHD.

**5.3 Experimental results**

**(1) Potential wells for different samples-**

The force field feature extraction based on potential wells was tested on the USTB ear database. However, the results show that different samples for the same subject possess different numbers and locations of potential wells. Fig. 5 shows the potential wells for the same subject with four different samples in the USTB ear database. Applying this method on the other subjects on the USTB ear database, the similar results were obtained. If there is illumination or pose change among different samples of the same subject, the potential wells are unstable. It is obvious that the potential wells for the same subject with different samples are various, so we cannot use the potential wells as the feature to identify different subjects.

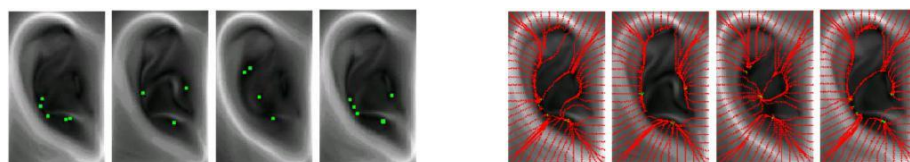


Fig. 5. Potential wells for the same subject. In the left four images, green points are potential wells for each ear sample . In the right four images, red curves are field lines formed by test pixels.

**(2) Effectiveness of the adaptive threshold segmentation-**

To test the effectiveness of our adaptive threshold segmentation for convergence images, this paper did contrast experiment both on the USTB ear database and the Spain database. Table 1 shows the concrete data.



**Table. 1. Results of adaptive threshold segmentation**

Ear databases	Total of samples	Correct numbers	Correct rate
USTB	308	300	97.4%
Spain	102	97	95.1%

The standard for right segmentation is that the binary image maintains useful information as much as possible while not brings in some interference information. Because only in this way can we ensure that the canny operator could extract the edge effectively and the noisy points would not disturb the calculation of the MHD. Table 1 shows that our method is effective since it almost realizes the automatic selection of threshold for each convergence image. However, there are still a small number of failed samples. For those failed samples, we have to choose the threshold by experiment.

**(3) Ear recognition based on the force field transform-**

In order to test the effect of our improved convergence-based ear recognition algorithm and the F+PCA+LDA method, we have applied them on two different databases. In the USTB database, we chose the first three ear samples of every subject as the training samples, and the last image was treated as the testing sample. In the Spain database, four images for each subject were randomly chosen as the training samples and the remainder two samples were testing samples. In

addition, classical methods like PCA and LDA for ear recognition were compared with our methods. Table 2 shows the experimental results.

As shown in the Table 2, F+PCA+LDA method has the highest recognition rate 98.7% of all the methods adopted in this paper. This proves that force field transform could improve the recognition rate. The improved convergence-based ear recognition method have higher ear recognition rates than the PCA and LDA on the Spain ear database. When tested on the USTB database, the recognition rates of our methods reduce a little but still not lower than the LDA and higher than the PCA.

From the data in the Table 2, we concluded that our methods have higher recognition rates than the other two methods. This is mainly because that our methods are based on the force field transform and the force value of one pixel with specific location is almost decided by the pixels nearby such location, therefore, they become less sensitive to the change in the illumination and pose. However, when the change is more obvious, especially when the gray values of the nearby pixels change a lot, the ear recognition rate will reduce. This explains why the recognition rates are lower in the USTB database than that in the Spain database when using our two methods.

**Table. 2. Comparison of different ear recognition methods**

Methods	Spain ear database	USTB ear database
PCA	82.4%	92.2%
PCA+LDA	88.2%	93.5%
Improved convergence-based ear recognition	100%	93.5%
F+PCA+LDA	100%	98.7%

**VI. CONCLUSION**

This paper researched three different applications of force field transform for ear recognition. One conclusion was that the potential wells were not suitable for ear recognition since it is very sensitive to the illumination and pose change. In the application of convergence field, this paper presented an improved convergence-based ear recognition algorithm which used the geometrical property of convergence field. It uses the adaptive threshold segmentation to translate the convergence images into binary images, which has improved the automation of the algorithm. During the classification process, Modified Hausdorff Distance was adopted to calculate the distance between different feature vectors extracted by the canny operator, so the computational complexity was reduced. Furthermore, the algebraic property of force field was also used for ear recognition. Experimental results prove that ear recognition combined with force field transform is effective, and both the geometrical property of convergence field and the algebraic property of force field are useful for ear recognition.

**REFERENCES**

- [1] B.Victor, K.Bowyer and S.Sarkar, "An Evaluation of Face and Ear Biometrics," *Proceedings of International Conference on Pattern Recognition*, 429-432 (2000).
- [2] Mu Zhichun, Yuan Li and Xu Zhengguang, "Shape and Structural Feature Based Ear Recognition," *The 5th Chinese Conference on Biometric Recognition, Guangzhou China*, 663-670 (2004).
- [3] D.J.Hurley, M.S.Nixon and J.N.Carter, "A New Force Field Transform for Ear and Face Recognition," *Proceeding of the IEEE International Conference of Image Processing*, 25-28(2000).
- [4] D.J.Hurley, M.S.Nixon and J.N.Carter, "Force Field Energy Functionals for Image Feature Extraction," *Image and Vision Computing*, 20:311-317 (2002).
- [5] D.J.Hurley, M.S.Nixon and J.N.Carter, "Force Field Feature Extraction for Ear Biometrics," *Computer Vision and Image Understanding*, 98:491-512 (2005).
- [6] D.P.Huttenlocher, G.A.Klanderma and W.J.Rucklidge, "Comparing Images Using the Hausdorff Distance," *IEEE Transactions on PAMI*, 15(9):850~863 (1993)
- [7] M.A.Carreira-Perpinan, *Compression Neural Networks for Feature Extraction: Application to Human Recognition from Ear Images*, Technical University of Madrid, Madrid, 1995